BIOCHEMISTRY
including biophysical chemistry & molecular biology

Article

pubs.acs.org/biochemistry

Detecting a Quasi-stable Imine Species on the Reaction Pathway of SHV-1 β-Lactamase and 6β-(Hydroxymethyl)penicillanic Acid Sulfone

Tao Che,[†] Elizabeth A. Rodkey,[†] Christopher R. Bethel,[⊥] Sivaprakash Shanmugam,[†] Zhe Ding,[†] Marianne Pusztai-Carey,[†] Michael Nottingham,[#] Weirui Chai,[#] John D. Buynak,[#] Robert A. Bonomo,[†,‡,§,∥,⊥] Focco van den Akker,[†] and Paul R. Carey*[,†]

[†]Department of Biochemistry, [‡]Department of Molecular Biology and Microbiology, [§]Department of Pharmacology, and [∥]Department of Medicine, Case Western Reserve University, Cleveland, Ohio 44106, United States

[⊥]Research Service, Louis Stokes Cleveland Veterans Affairs Medical Center, Cleveland, Ohio 44106, United States

[#]Department of Chemistry, Southern Methodist University, Dallas, Texas 75275, United States

Supporting Information

ABSTRACT: For the class A β-lactamase SHV-1, the kinetic and mechanistic properties of the clinically used inhibitor sulbactam are compared with the sulbactam analog substituted in its 6β position by a CH_2OH group (6β-(hydroxymethyl)-penicillanic acid). The 6β substitution improves both *in vitro* and microbiological inhibitory properties of sulbactam. Base hydrolysis of both compounds was studied by Raman and NMR spectroscopies and showed that lactam ring opening is followed by fragmentation of the dioxothiazolidine ring leading to formation of the iminium ion within 3 min. The iminium ion slowly loses a proton and converts to *cis*-enamine (which is a β-aminoacrylate) in 1 h for sulbactam and in 4 h for 6β-(hydroxymethyl) sulbactam. Rapid mix−rapid freeze Raman spectroscopy was used to follow the reactions between the two sulfones and SHV-1. Within 23 ms, a 10-fold excess of sulbactam was entirely hydrolyzed to give a *cis*-enamine product. In contrast, the 6β-(hydroxymethyl) sulbactam formed longer-lived acyl−enzyme intermediates that are a mixture of imine and enamines. Single crystal Raman studies, soaking in and washing out unreacted substrates, revealed stable populations of imine and *trans*-enamine acyl enzymes. The corresponding X-ray crystallographic data are consonant with the Raman data and also reveal the role played by the 6β-hydroxymethyl group in retarding hydrolysis of the acyl enzymes. The 6β-hydroxymethyl group sterically hinders approach of the water molecule as well as restraining the side chain of E166 that facilitates hydrolysis.

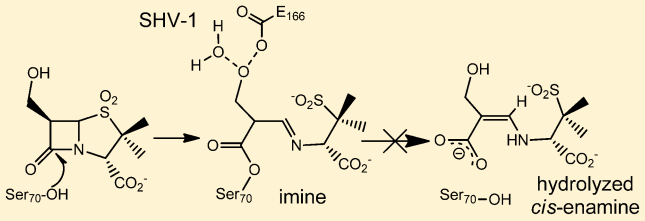

The production of β-lactamases is the major cause of failure of β-lactam-based therapy against Gram-negative bacteria. Since the first β-lactamase was identified in *Bacillus* (*Escherichia*) *coli* >70 years ago,[1] more than 1400 different enzymes have been reported. Currently, β-lactamases are grouped into four classes (A through D) based on the Ambler classification.[2] New β-lactamases generated in the Enterobacteriaceae family, the *Pseudomonas*, *Acinetobacter*, and *Klebsiella* genera, stimulated the development of novel β-lactam antibiotics from penicillins to extended-spectrum cephalosporins (e.g., ceftazidime, ceftriaxone, and cefepime) and to carbapenems (imipenem, meropenem, ertapenem, and doripenem). Regrettably, an emerging number of community and hospital-acquired *E. coli* and *K. pneumoniae* have already shown resistance to this last-line of defense (cephalosporins and carbapenems).[3] An urgent need exists to design more effective therapies.

In most clinical applications, mechanism-based inhibitors (clavulanate, sulbactam, or tazobactam) against β-lactamases are applied in combination with a partner β-lactam antibiotic. The inhibition mechanism of these inhibitors has been widely studied.[4] When the inhibitors react with the target β-lactamase, the carbonyl carbon of the β-lactam ring is attacked by a Ser-OH forming an acyl−enzyme followed by the opening of the adjacent dioxothiazolidine ring. Study of the reaction pathways postulates that an iminium ion (often referred to as an imine) intermediate is then rapidly formed that tautomerizes to an enamine. The latter often forms a stable acyl−enzyme complex and inhibits the enzyme. The structures of acyl−enzyme complexes have been solved showing that a *trans*-enamine is covalently bound to the active site.[5,6] This finding led to new inhibitor design aimed at producing a more stable *trans*-enamine in the active site. SA2-13, a penam sulfone derivative, is one such structure-based inhibitor that can stabilize the *trans*-enamine intermediate to inhibit class A β-lactamases.[7] However, commercial inhibitors narrowly target the class A enzymes. New clinically useful β-lactamase inhibitors need to have a significantly broader inhibitory spectrum, ideally targeting all serine β-lactamases (classes A, C, and D). Recent studies with avibactam, a diazabicyclooctane (DBO) inhibitor

Received: September 23, 2014
Revised: December 22, 2014
Published: December 23, 2014

DOI: 10.1021/bi501197t
Biochemistry 2015, 54, 734−743

of the non-β-lactam class, support the importance of this strategy.

In 1999, Bitha et al. showed that the addition of a 6-hydroxymethyl group in sulbactam improves the activity against both TEM-1 (175-fold increase) and AmpC (57-fold increase) β-lactamases.[8,9] This 6β-hydroxymethyl sulbactam (PSR-3-283A) also restores the activity of piperacillin *in vitro* (MIC) and *in vivo* (ED_{50}) against both class A and class C β-lactamase producing microorganisms. Bitha et al. proposed that the approach of the hydrolytic water may be affected by the presence of 6β-hydroxymethyl group. In 2012, Papp-Wallace et al.[10] investigated the reaction pathway of PSR-3-283A with TEM-1 and PDC-3, the AmpC of the pathogen *Pseudomonas aeruginosa*, using mass-spectrometry. Their results indicate that the improved efficiency of PSR-3-283A may be due to loss of the hydrolytic water after acylation. However, the underlying mechanism was not studied in detail, partly because the reaction occurs very quickly.

Recently, our laboratory developed a new protocol to study this rapid reaction. This approach combines rapid mix–rapid freeze with Raman spectroscopy enabling us to capture the intermediates or products on the millisecond time frame.[11] The rapid reaction–Raman approach has the advantage that it provides time-resolved structural data. Herein, using this new protocol, we tested PSR-3-283A with the clinically important β-lactamase, SHV-1, one of the most common class A β-lactamases detected in clinical isolates of *E. coli* and *K. pneumoniae*. By comparing PSR-3-283A with sulbactam, we show that a large population of imine species is formed as a relatively stable intermediate in the reaction between PSR-3-283A and SHV-1, but only hydrolyzed *cis*-enamine product is detected with sulbactam. This is the first time we have captured a quasi-stable imine in the active site because with the commercial inhibitors, the imine intermediate is usually very short-lived. A crystal structure of SHV-1 in complex with PSR-3-283A shows the 6-hydroxymethyl group in the imine and enamine complex forms extra H-bonds with the deacylation water molecule and the general base E166 and therefore hampers deacylation. The different properties between sulbactam and PSR-3-283A due to the additional 6β-hydroxymethyl group provide an approach to improving or designing more versatile β-lactamase inhibitors.

MATERIALS AND METHODS

Antibiotics and β-Lactamase Inhibitors. The antibiotics used in this study were obtained from their respective manufacturers as indicated: ampicillin, cephalothin, and clavulanic acid, potassium salt, from Sigma (St. Louis, MO); sulbactam, sodium salt, from Pfizer (Groton, CT); tazobactam, sodium salt, from Chem-IMPEX (Wood Dale, IL); and nitrocefin from Becton Dickinson (Franklin Lakes, NJ). The sodium salt of PSR-3-283A (263 Da) and 6-D,D-sulbactam were synthesized in the laboratory of John D. Buynak. Chemical structures of β-lactamase inhibitors are represented in Figure 1.

Subcloning, Expression, and Purification. The subcloning, expression, and purification of wild-type (wt) SHV-1 was carried out similarly to that previously described.[12−14] Briefly, the bla_{SHV-1} gene was subcloned into the phagemid vector pBC SK(−) (Stratagene) with a periplasmic leader sequence. This construct was transformed into *Escherichia coli* DH10B cells (Stratagene). Cells were grown overnight in lysogeny broth (LB) supplemented with 20 μg/mL chloramphenicol. Cells

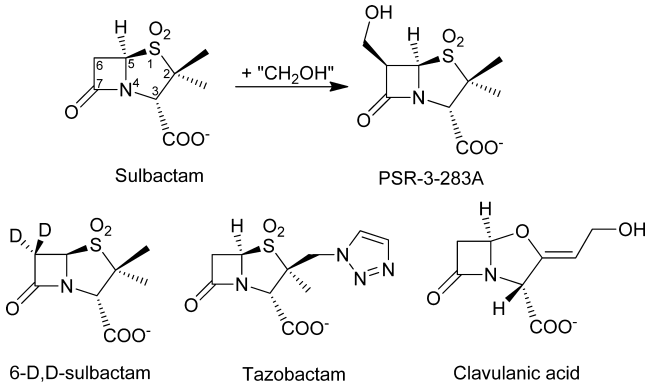

Figure 1. Chemical structures of the clinical inhibitors, tazobactam, sulbactam, and clavulanic acid, and PSR-3-283A.

were lysed using a periplasmic lysis protocol adapted from Peripreps Periplasting Kit (EpiCentre). Briefly, cell pellets are resuspended in a buffer containing 200 mM Tris-HCl, pH 7.5, 20% sucrose, 1 mM EDTA, and 4 mg/g dry cell weight lysozyme. After a 5 min incubation without stirring, the reaction is diluted 1.5-fold with water and left on ice for 7 min. The lysate is cleared by centrifugation (12000*g*) at 4 °C for 15 min. The lysate was subsequently purified using preparative isoelectric focusing (pIEF) gel chromatography. β-Lactamase was detected using nitrocefin (Calbiochem), a chromogenic β-lactamase substrate. Nitrocefin "positive" pIEF fractions were applied to a Q-Sepharose anion exchange column using either 20 mM HEPES, pH 7.0, or 20 mM BisTris, pH 6.5, as the equilibration buffer with 1 M NaCl or 1 M KCl added as the elution buffer. In both the HEPES/NaCl and BisTris/KCl conditions, the β-lactamase eluted in the flow-through while the majority of impurities bound the column. β-lactamase positive fractions were applied to a Superdex75 gel filtration column as the final purification step. Protein purity was assessed by SDS-PAGE, and pure protein was concentrated to 5 mg/mL.

Kinetics. Steady state kinetics were performed on an Agilent 8453 diode array spectrophotometer (Palo Alto, CA) in 10 mM phosphate-buffered saline (pH 7.4). V_{max} and K_m were determined from initial steady-state velocities for nitrocefin (NCF), $\Delta\varepsilon_{482}$ =17,400 $M^{-1}cm^{-1}$. The kinetic parameters were obtained using iterative nonlinear least-squares fit of the data to the Henri–Michaelis equation using Origin 8.0 (OriginLab, Northampton, MA) according to eq 1:

$$v = V_{max}[S]/(K_m + [S]) \quad (1)$$

IC_{50}, defined as the inhibitor concentration resulting in a reduction of NCF (100 μM) hydrolysis by 50%, was determined by measurements of initial velocities after 5 min preincubation of enzyme with inhibitor.[15] The first-order rate constant for enzyme inactivation, k_{inact}, was determined by monitoring the reaction time courses in the presence of increasing concentrations of inactivators. A fixed concentration of enzyme, nitrocefin, and increasing concentrations of inactivator were used in each assay. The k_{obs} for inactivation was determined graphically as the reciprocal of the ordinate of the intersection of the straight lines obtained from the initial, v_0, and final, v_f, steady-state velocities. Each k_{obs} was plotted versus inhibitor concentration, I, and fit to eq 2 to determine k_{inact} and k_{inact}/K_I (the second order rate constant for reaction of free enzyme with free inhibitor to give inactive enzyme):

DOI: 10.1021/bi501197t
Biochemistry 2015, 54, 734−743

$$k_{obs} = k_{inact}[I]/(K_I + [I]) \quad (2)$$

Partition ratios (k_{cat}/k_{inact}) were determined as the ratio of inhibitor concentration to enzyme concentration that was necessary to decrease the enzyme activity by 95%. Partition ratios were determined after a 24 h incubation with increasing concentrations of the inhibitor. Incubations were done in a final volume of 300 μL, and 25 μL of this reaction mixture was added to a 1 mL final volume to determine the residual enzyme activity using 100 μM nitrocefin.

Susceptibility Testing. For disc diffusion testing, *E. coli* DH10B pBC SK(−) with and without bla_{SHV-1} were used. Disc diffusion assays were conducted using the guidelines of Clinical and Laboratory Standards Institute (CLSI).[16] Solutions of cephalothin (30 μg) and inhibitor (30 μg) were pipetted onto discs based on the combinations shown in Table 2 and allowed to dry for 1 h. Colonies were directly resuspended into sterile water equivalent to a 0.5 McFarland standard and used to inoculate Mueller Hinton (MH) agar plates. The discs were carefully placed on each plate. The bacteria were grown at 37 °C for 18 h, and zone diameters were measured.

Raman Studies in Solution. For the rapid mix−rapid freeze experiment, we used a slightly modified KinTek instrument model RQF-3. Reactions were initiated by mixing SHV-1 enzyme (5 mg/mL in 2 mM HEPES, pH 7) with β-lactamase inhibitors (sulbactam, 6-D,D-sulbactam, PSR-3-283A) in a 1:10 molar ratio. The mixture then traversed through different reaction loops with predetermined time delay, and the reaction mixture was rapidly frozen by injection into isopentane at about −110 °C within a tube that was immersed in liquid nitrogen. Isopentane was removed from the ice, and by freeze-drying the frozen material, the lyophilized powder was obtained that constituted Raman samples. The powder was examined using the Raman microscope[17] (80 mW of 647.1 nm was used as the excitation source, and each data set was acquired using 1 × 100 s exposure). On the basis of the reaction loops and exit line volume (which determine the distance of travel for the mixture of enzyme and substrate prior to freezing) and the rpm of the drive motor, we calculated the time of the reaction. The reaction mixture travels 1−2 cm in the air after the exit loop to enter the cold isopentane. This gap can produce the error in the time points between 1 to 3 ms based on the rpm of the drive motor. A schematic picture of rapid mix−rapid freeze has been described previously.[11]

Crystallization and Soaking. Crystals of wt SHV-1 β-lactamase were grown using hanging drop vapor diffusion over a well solution containing 21−30% PEG6000 and 0.1 M HEPES, pH 6.8−8.2. The protein solution (5 mg/mL) was combined with the Cymal-6 additive (Hampton, final concentration 0.56 mM). Five microliter drops were set using a 1:1 protein/well solution ratio with crystals growing in 1−3 weeks. Crystals were soaked in a drop containing mother liquor and 50 mM PSR-3-283A for 15 min. After soaking, crystals were transferred to a cryoprotectant solution containing mother liquor and inhibitor supplemented with 25% methyl-2,4-pentanediol (MPD) before being flash frozen in liquid nitrogen.

Data Collection and Refinement. All data were collected on BL9-2 at the Stanford Synchrotron Radiation Lightsource (SSRL), Stanford University, Menlo Park, CA. Data were integrated and scaled using HKL2000.[18] Structures were determined by isomorphous replacement using the wt SHV-1 apo structure (PDB ID: 1SHV). Restrained refinement was carried out using REFMAC5,[19] and COOT[20] was used for model building and manual refinement. Cymal-6 detergent molecules were included in the refinement. After refinement of side chains and addition of solvent molecules, difference electron density was present for part of the PSR-3-283A inhibitor bound in the active site. Inhibitor coordinate and topology files were generated using PRODRG server.[21] The inhibitor was modeled in a linearized, extended conformation with the tail atoms being less ordered. The more electron-dense sulfone moiety of the inhibitor was modeled into the strongest difference density (6.5σ) in this region. Data collection and refinement statistics are found in Table 1. RMSDs were calculated using the LSQKAB utility in CCP4.[22]

Table 1. X-ray Data Collection and Refinement Statistics for SHV-1 PSR-3−283A complex

Data Collection Statistics	
space group	$P2_12_12_1$
cell dimensions	
a, *b*, *c* (Å)	49.2, 55.3, 84.5
α, β, γ (Å)	90.0, 90.0, 90.0
wavelength (Å)	0.9795
resolution (Å^2)	1.37
R_{sym}	0.035(0.273)
$I/\sigma I$	28.3(4.1)
completeness (%)	98.6(94.7)
redundancy	3.5(3.1)
Refinement Statistics	
resolution range (Å)	27.7−1.37
no. of reflns	46331
R_{work}/R_{free}	0.130/0.172
no. of atoms (protein/ligand/water)	2106/62/269
RMSD	
bond length (Å)	0.010
bond angle (deg)	1.36
avg B-factors (Å^2)	
protein	15.2
ligands	25.5
water	30.0
Ramachandran plot statistics (%)	
core	92.6
allowed regions	6.9
gen. allowed regions	0.4
outliers	0.0

RESULTS

Kinetic Parameters. The kinetic parameters for PSR-3-283A with the target enzyme SHV-1 β-lactamase were measured, and the results are compared in Table 2 with those for the clinically used inhibitors tazobactam, sulbactam, and clavulanate.

The observed IC_{50} (0.32 ± 0.03 μM) of PSR-3-283A is 10-fold and 3-fold higher than those of tazobactam (0.030 ± 0.003 μM) and clavulanate (0.10 ± 0.02 μM), respectively. However, it is 10-fold lower than that of sulbactam (3.4 ± 0.5 μM). Additionally, the K_I (0.56 ± 0.05 μM) is about 3-fold higher than that of tazobactam (0.16 ± 0.03 μM) but 3-fold lower than those of clavulanate (2.0 ± 0.2 μM) and sulbactam (1.5 ± 0.3 μM), respectively. This indicates that PSR-3-283A has a higher affinity compared with clavulanate or sulbactam for SHV-1. The k_{inact}/K_I ratio for PSR-3-283A is comparable to that of clavulanate and 4-fold higher than that of sulbactam.

DOI: 10.1021/bi501197t
Biochemistry 2015, 54, 734−743

Table 2. Kinetic Parameters of SHV-1 β-Lactamase with Various Inhibitors

	IC_{50}(5 min) (μM)	k_{inact} (s^{-1})	K_I (μM)	k_{inact}/K_I (μM^{-1} s^{-1})	k_{cat}/k_{inact} (24 h)
clavulanic acid	0.10 ± 0.02	0.034 ± 0.001	2.0 ± 0.2	0.017 ± 0.002	40
tazobactam	0.030 ± 0.003	0.10 ± 0.01	0.22 ± 0.03	0.45 ± 0.07	60[a]
PSR-3-283A	0.32 ± 0.03	0.010 ± 0.001	0.56 ± 0.05	0.018 ± 0.002	80
sulbactam	3.4 ± 0.5	0.006 ± 0.001	1.5 ± 0.3	0.004 ± 0.001	10000

[a]Previously reported as 5. Difference likely due to potency of the product.

The partition ratio at 24 h for PSR-3-283A (t_n = 80) is comparable to those of tazobactam (t_n = 60) and clavulanate (t_n = 40) and at least 100-fold lower than that of sulbactam (t_n = 10000). The kinetic data with SHV-1 β-lactamase show that PSR-3-283A has not only increased affinity but also greater inactivation efficiency compared with sulbactam. This is likely attributable to the additional 6-hydroxymethyl group in PSR-3-283A and its ability to resist catalysis.

Susceptibility Testing. In order to test PSR-3-283A's ability to synergistically help antibiotics kill bacterial cells, disc diffusion assays were conducted and zone diameters were measured for *E. coli* DH10B without or with pBC SK(−) bla_{SHV-1} (Table 3). The *E. coli* strain expressing SHV-1 was resistant to the antibiotic cephalothin with a zone size of 6 mm. When cephalothin was combined with clinical inhibitors or PSR-3-283A, the latter displayed slightly better synergy (24 mm) than tazobactam (16 mm) and much better than sulbactam (10 mm).

Table 3. Disc Diffusion Assays

	zone diameter (mm)	
	E. coli DH10B pBCSK control	*E. coli* DH10B pBCSK SHV-1
cephalothin[a]	34	6
cephalothin−sulbactam[a]	34	10
cephalothin−clavulanic acid[a]	34	36
cephalothin−tazobactam[a]	36	16
cephalothin−PSR-3-283A[a]	40	24

[a]Cephalothin (30 μg) and 30 μg of each inhibitor were used.

Base Hydrolysis. Before investigating the enzyme catalyzed reactions of PSR-3-283A and sulbactam, we followed base hydrolysis of the two inhibitors by normal Raman spectroscopy to aid us in understanding the mechanism of inactivation of β-lactamases. The involvement of a serine hydroxy function in the enzyme reaction has prompted researchers to employ parallel base hydrolysis to study rearrangement of β-lactamase inhibitors.[23] Herein, the results can be understood in terms of Scheme 1. The major Raman peak assignments follow those we have derived in order to characterize imine and enamine species in the active site of SHV-1 β-lactamase.[4] The key assignments are listed in Table 4.

Table 4. Peak Assignment Derived from Gaussian Calculations

	species	wavenumber (cm^{-1})	peak assignments
	unreacted sulbactam	1789	ν(C═O) of β-lactam ring
		1402	ν(−CO_2^-) stretch at C3
		631	ν(−C−S) between S1 and C5
base catalysis	sulbactam (30 min)	1630	ν(C═N) of deprotonated imine
		1581	ν(C═C) of *cis*-enamine
		1402	ν(−CO_2^-) stretch at C3 and C7
		600/536	ν(−SO_2^-)
	PSR-3-283A (30 min)	1631	ν(C═N) of deprotonated imine
		1594	ν(C═C) of *cis*-enamine
		1403	ν(−CO_2^-) stretch at C3 and C7
		597/538	ν(−SO_2^-)
SHV-1 catalysis	sulbactam (23 ms)	1588	ν(C═C) of *cis*-enamine
		556	ν(−SO_2H) of *cis*-enamine
	PSR-3-283A (23 ms)	1780	ν(C═O) of β-lactam ring
		1630	ν(C═N) of deprotonated imine
		1612	ν(C═C) of *trans*-enamine
		1586	ν(C═C) of *cis*-enamine
		555	ν(−SO_2H) of enamine

Previous work in our laboratory by Kalp et al.[4] studied the detailed mechanisms when sulbactam, clauvalanate, or tazobactam react with SHV-1 within a crystal. Much effort has been expended to assign the Raman peaks of imine and *cis*- and *trans*-enamine species in the reaction pathway. Using a biochemical reagent or isotopic substitutions, Kalp et al. provide solid evidence showing that protonated imine (C═NH^+) has a characteristic peak near 1656 cm^{-1}, *trans*-enamine (C═C) near 1595−1615 cm^{-1}, and *cis*-enamine (C═C) near 1580−1595 cm^{-1} where the assignments are stretching modes with a large contribution from the double bond. These

Scheme 1. Mechanism of Base Catalyzed Hydrolysis

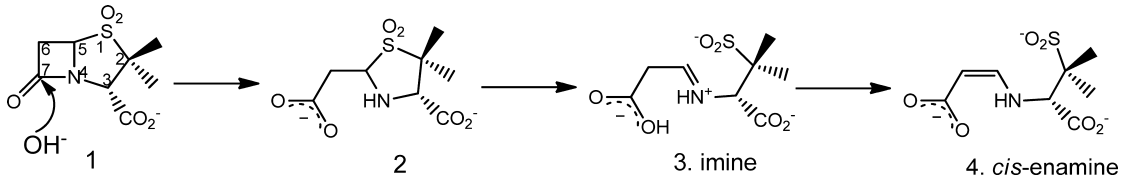

DOI: 10.1021/bi501197t
Biochemistry 2015, 54, 734−743

assignments are also strongly supported by Kalp's and our recent quantum mechanical calculations using the Gaussian program. Taken together, these constitute the foundation for our assignments in the base hydrolysis studies and reactions of PSR-3-283A and SHV-1.

In the base hydrolysis experiment, 2 μL of 20 mM sulbactam was mixed with 2 μL of 1 M NaOH, and the Raman spectra were then recorded in real time. In Figure 2A, the reaction

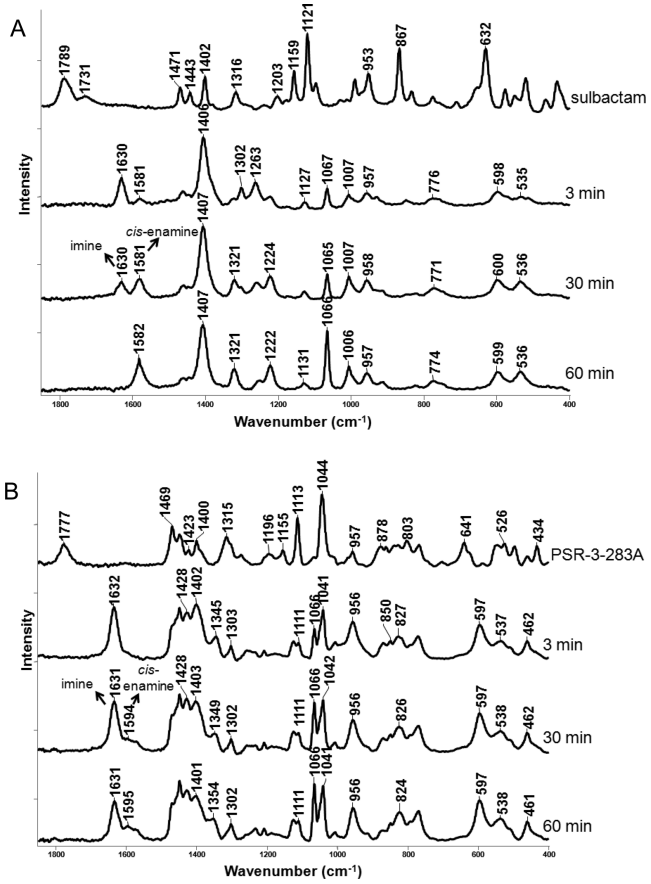

Figure 2. Base hydrolysis of sulbactam and PSR-3-283A. Two microliters of 5 mg/mL sulbactam (A) or 5 mg/mL PSR-3-283A (B) were incubated with 2 μL of 1 M NaOH at room temperature. The reaction was recorded immediately after the incubation began using Raman spectroscopy.

appears to display a strict two-step mechanism. After sulbactam and NaOH were mixed, the OH^- attacks the carbonyl group in the β-lactam ring and the imine rapidly accumulates and reaches a maximum at less than 3 min, as evidenced by the intense peak at 1630 cm^{-1}. The 1630 cm^{-1} peak, based on Gaussian calculations,[24] is assigned to C═N in the deprotonated imine (Scheme 1, Table 4) Opening of the five-membered ring is supported by the absence of the 632 cm^{-1} peak (C_5–S_1 stretch). The appearance of the profile at 598/535 cm^{-1} originates from the deprotonated $-SO_2^-$[25,26] in the hydrolyzed imine and *cis*-enamine species (**3** and **4**, Scheme 1). The accumulation of imine at 3 min also means that the rate-limiting step is the transition from imine to enamine. From 3 to 60 min, the peak at 1630 cm^{-1} decreases, while the 1581 cm^{-1} feature continues to increase, indicating that more hydrolyzed *cis*-enamine is formed (Table 4). At 60 min, all imine molecules have been converted to *cis*-enamine. This two-step reaction is also supported by the NMR analysis (Figure S1, Supporting Information). In Supporting Information, for base hydrolysis, we assign resonances in the ^{1}H NMR to imine and *cis*-enamine isomers. They interconvert with the same time dependence that we have characterized in the base hydrolysis measured by Raman analysis.

In the hydrolysis of PSR-3-283A by 1 M NaOH (Figure 2B), the reaction displays a similar two-step mechanism but the imine–enamine tautomerization rate is eight times slower than that in sulbactam. At 3 min, all PSR-3-283A molecules are hydrolyzed to imine species (1632 cm^{-1}), and the latter still dominates at 1 h. After 4 h, the ratio of imine/enamine (1631:1595 cm^{-1}) is ~1:1 (data not shown). Thus, for PSR-3-283A undergoing base hydrolysis, the imine species requires a higher energy barrier for conversion to enamine compared with that for the sulbactam derived imine and enamine. There are two possible explanations for this slow conversion. One is that the bulky $-CH_2OH$ replaces one of the two hydrogen atoms, thus essentially reducing the rate by half; the other is that the $-CH_2OH$ group interferes with the approach of a OH^- base to the remaining hydrogen at C6 position, slowing the overall process. The imine is important because in the following sections we will show how its stability is increased further in SHV-1 β-lactamase's active site by interactions with the 6-hydroxymethyl.

Raman Studies of Reactions with SHV-1 in Solution. In order to compare the inhibition mechanisms of the β-lactamase between sulbactam and PSR-3-283A, we utilized rapid mix–rapid freeze combined with Raman microspectroscopy to monitor the intermediates and products formed in their reaction pathways. Sulbactam or PSR-3-283A was incubated with SHV-1 at the ratio of 1:10 (E/I), and the reaction was quenched by liquid pentane immersed in liquid nitrogen at different time points (23 ms to 5 s). The quench temperature was approximately −110 °C. Figure 3A shows the reaction of SHV-1 with sulbactam (E/I = 1:10). The characteristic substrate Raman peak (1789 cm^{-1}) is assigned to the carbonyl group (C═O) in the β-lactam ring.

In the difference spectrum after mixing, this peak completely disappears at 23 ms indicating that all the sulbactam molecules are hydrolyzed by SHV-1. The substrate peaks are replaced mainly by a new peak that is designated as the *cis*-enamine (1586 cm^{-1}) in the reaction pathway (species **4**, Scheme 2, Table 4).[4] This peak originates from the coupled C═C stretch mode in *cis*-enamine (Table 4). Both the disappearance of the 631 cm^{-1} peak (C_5–S_1 group) and the new profile at 602/556 cm^{-1}, assigned to the $-SO_2H$ group (since now the pH is ~7.0 and the 600/535 cm^{-1} profile for $-SO_2^-$ is replaced by the 602/555 cm^{-1} profile for $-SO_2H$), indicate the opening of the five-membered ring. The enzyme remained fully active against nitrocefin (a colorimetric substrate of β-lactamase),[27] indicating that the *cis*-enamine species is a hydrolyzed product and there is no acyl–enzyme complex in Figure 3A.

Figure 3B shows the results for the freeze quenched species formed by the reaction between SHV-1 and PSR-3-283A (E/I = 1:10). Three unresolved peaks (1630, 1612, and 1586 cm^{-1}) at 23 ms are assigned to acyl–enzyme complexes made up of populations of species **3**, **5**, and **6** in Scheme 2 although extensive band overlap precludes definitive assignments. In this analysis, the 1630 cm^{-1} peak is equivalent to the 1632 cm^{-1} in Figure 2B, which is assigned to the deprotonated imine (−C═N−); peaks at 1612 and 1586 cm^{-1} correspond to the *trans* and *cis*-enamine, respectively (Table 4). The appearance of the completed spectral profile at 23 ms spectrum indicates that

DOI: 10.1021/bi501197t
Biochemistry 2015, 54, 734–743

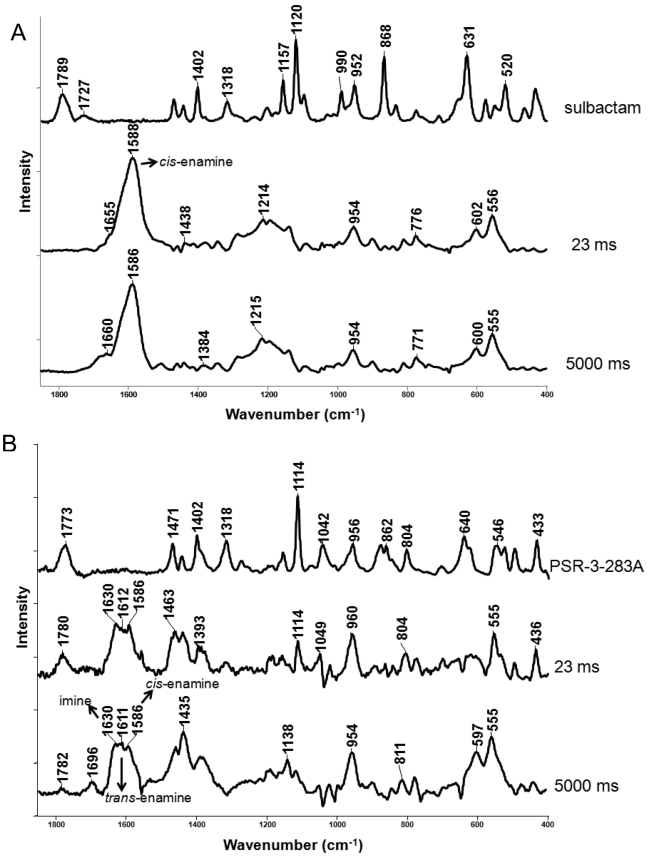

Figure 3. Raman studies of reactions with SHV-1 in solution. The SHV-1 (2 mg/mL) was mixed with sulbactam (A) or PSR-3−283A (B) at the molar ration of 1:10 (E/I). Using the KinTek device, the reaction was quenched at different time points from 23 ms to 1 min. The quenched samples were then freezed-dried, and their Raman spectra were recorded.

acylation rate is fast for PSR-3-283A. However, the deacylation rate is much slower than that for sulbactam because the peak at 1780 cm^{-1} that represents C═O stretch in the intact β-lactam ring is still evident at 23 ms and to a small extent at 5 s. The 1696 cm^{-1} band seen at 5 s is due to the coupled C═O stretch from the conjugated acryloyl species (−C═C−C(═O)−O−) in acyl−enzyme complexes **5** and **6** (Scheme 2).[28,29] At 5 s, growing intensity of the 597/555 cm^{-1} profile ($-SO_2H$ in species **4**, Scheme 2), as well as the decrease of 1782 cm^{-1} peak (C═O in β-lactam ring), suggests that several turnovers have occurred and some of the acyl−enzyme complexes at 23 ms are hydrolyzed and released as products. At 23 ms, the 597/555 cm^{-1} is of low intensity, which reinforces the conclusion that a population of unreacted inhibitor remains. Once product is released, the $-SO_2H$ population increases and generates the more intense profile at 597/555 cm^{-1}. However, a substantial population of imine species (1630 cm^{-1}, Table 4) remains at 5 s, which is believed to covalently bind to the active site of SHV-1 and inhibit the enzyme. The presence of a relatively stable acyl−enzyme is supported by the unreacted PSR-3-283A peak at 1782 cm^{-1} (Figure 3B), as well as a nitrocefin assay showing that nitrocefin was not hydrolyzed by the enzyme.

The base hydrolysis data show that interconversion between the imine and enamine product is slow, 20−40 min, for both sulbactam and PSR-3-283A (Figure 2). However, in Figure 3A for SHV-1 catalysis of sulbactam, the prevalence of *cis*-enamine product means that very rapid imine-to-enamine interconversion has occurred in the active site, likely catalyzed by E166[30] followed by hydrolysis of the acyl−enzyme. Similarly, for PSR-3-283A, the mixture of imine and enamine in the acyl−enzyme population is maintained in the product mix indicating that hydrolysis of both acyl−enzyme species occurs at similar rates. Figure 3 demonstrates that PSR-3-283A makes a more stable acyl−enzyme population than sulbactam since it is stable for more than 10 min compared with less than 23 ms for sulbactam. Again, considering the base hydrolysis data, we do not expect enamine to imine interchange to occur when PSR-3-283A product is released from SHV-1.

X-ray and Raman Analysis of Single Crystals. From the kinetic and solution Raman results, we conclude that PSR-3-283A is a more effective inhibitor than sulbactam because its deacylation rate is much slower than that for the sulbactam derived species; it forms the relatively stable inhibited acyl−enzyme complexes that are likely a mixture of imines and enamines. We now provide a rationale from the structural analysis to show how the 6-hydroxymethyl group in PSR-3-283A increases acyl−enzyme stability.

Soaking PSR-3-283A into crystals of SHV-1 had a minimal effect on the structure of the enzyme. Superpositioning of all Cα atoms of the inhibitor complex onto the apo wt SHV-1 high resolution structure (PDB id 4FH4) yields a low rmsd of 0.144 Å indicating that the overall structure was essentially unaffected

Scheme 2. Proposed Reaction Mechanism for PSR-3-283A or Sulbactam with SHV-1

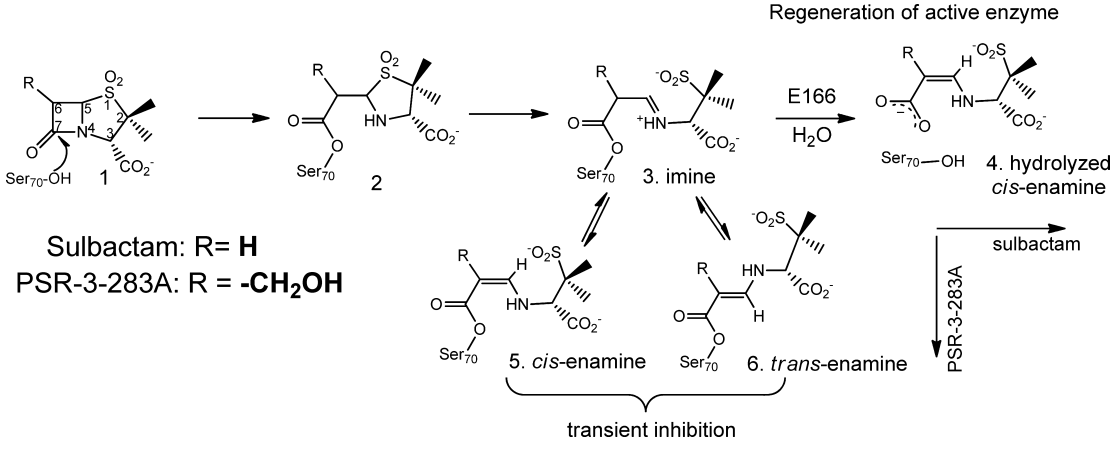

DOI: 10.1021/bi501197t
Biochemistry 2015, 54, 734−743

by inhibitor binding. The acyl region C7−C6−C5−N4 has well-defined electron density (Figure 4A) with the C7−C6−C5−N4 torsion angle being −179.4°. Thus, the C7 and N4 atoms are in the *trans* position. This shows that either the imine (species **3**, Scheme 2) or *trans*-enamine (species **6**, Scheme 2) has been trapped in the active site. The spectroscopic evidence above favors a mix of imine and enamine species. The tail region of PSR-3-283A beyond the carboxylate moiety does not seem well ordered (Figure 4A). The electron density after the carboxylate is broken although there is strong 6.5σ $F_o - F_c$ difference density in the vicinity likely representing the electron-dense sulfone moiety of PSR-3-283A.

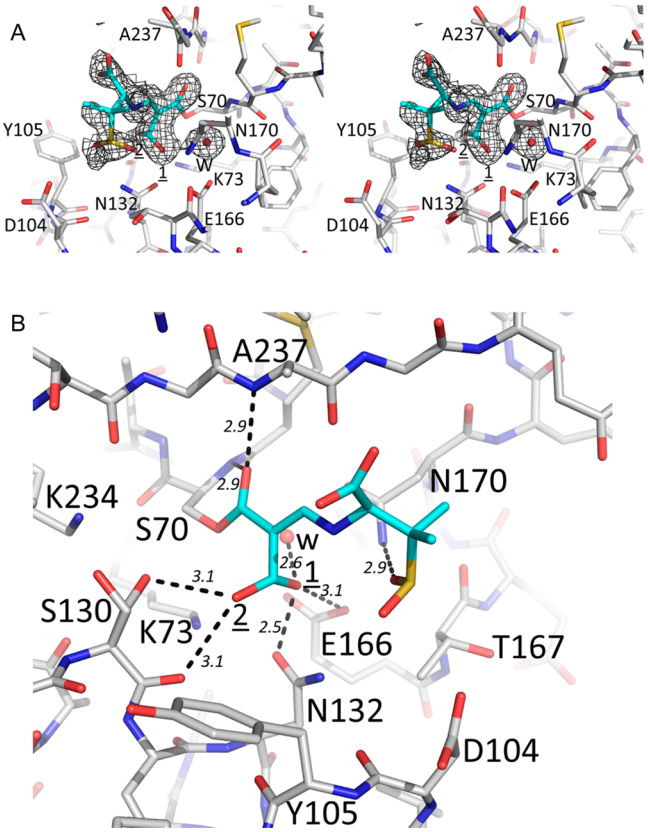

Figure 4. PSR-3-283A bound to SHV-1 active site. (A) Stereofigure of electron density $|F_o| - |F_c|$ difference density of PSR-3-283A with PSR-3-283A and deacylation water (labeled W) not included in refinement. Electron density is contoured at 3.25σ. Alternate conformations for the 6α-OH moiety are labeled by 1 and 2. (B) Interactions of PSR-3-283A in the active site. Hydrogen bonds are depicted as dashed lines with hydrogen bond distances shown. The deacylation water is labeled W.

The inhibitor is covalently bound via its C7 atom to Oγ of S70; the carbonyl oxygen atom of the inhibitor is situated in the oxyanion hole (formed by the backbone nitrogen H's of residues 70 and 237). The C6 hydroxyl atom has two conformations (Figure 4B). Optimization of B-factors suggested a mixture of conformation for the 6-hydroxymethyl group with form **1** predominating. The main conformation, labeled 1, has the hydroxyl pointed toward the deacylation water pocket. Crucially, in this position, the hydroxyl moiety hydrogen bonds with the deacylation water and also with E166 and N132 (Figure 4B). It is known that E166 acts as a general base to hydrolyze the substrate via the interposing deacylation water molecule. Here, the formation of the two hydrogen bonds with the water molecule and E166 may impair the function of E166, hindering it from activating that water molecule to hydrolyze the imine/enamine species formed by PSR-3-283A. It has been proposed that E166 acts as a general base to promote imine to enamine tautomerization.[30] The bond between E166's side chain and the -CH_2OH hydroxyl group will also interfere with this function and provides additional evidence as to why transformation from imine to enamine is incomplete for the acyl enzyme formed from 6β-hydroxymethyl sulbactam.

The second conformation of this C6 hydroxyl atom, labeled 2 with a smaller degree of occupancy, hydrogen bonds with the backbone oxygen of S130 in one of the conformers of the S130 side chain (Figure 4B). In addition, one of the oxygen atoms of the sulfone moiety of PSR-3-283A is within hydrogen bonding distance with H (NH_2) of the N170 side chain.

In order to compare the X-ray and Raman data directly, we undertook a single crystal Raman experiment running the reaction by soaking in PSR-3-283A. After PSR-3-283A was soaked in the holding solution containing a SHV-1 single crystal, intense peaks at 1630 cm^{-1} (imine species in Figures 2 and 3) and near 1608 cm^{-1} were detected (Figure 5). This indicates a mixture of imine and *trans*-enamine (Table 4). Considering from the Raman data that there was still unreacted PSR-3-283A present due to nonspecific binding, we performed a soakout experiment. After a SHV-1 single crystal was incubated with PSR-3-283A for 15 min, it was transferred to a fresh drop that does not contain any PSR-3-283A. After 15 min soakout, the unreacted PSR-3-283A was washed away (the 1777 cm^{-1} peak was now absent), but the 1630 and 1607 cm^{-1} peaks remained (Figure 5), indicating that the imine and *trans*-enamine species are covalently bound to the active site and inhibit the enzyme.

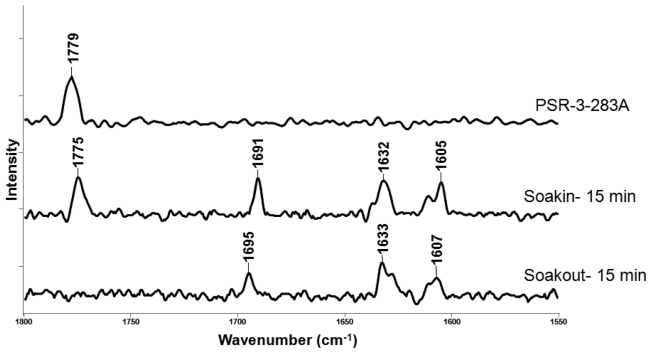

Figure 5. Soak-in and soak-out reactions of PSR-3-283A in crystals of SHV-1. One microliter of 20 mM PSR-3-283A was added to 4 μL of holding solutions containing a SHV-1 crystal. Raman spectra were recorded at different time points. After 15 min, the crystal was transferred to a fresh drop that did not contain the PSR-3-283A inhibitor. Raman spectra were taken at different time points. The spectra shown in the figure are 15 min after PSR-3-283A was soaked in (middle) and 15 min after the SHV-1 crystal was transferred out to the holding solution (bottom).

The Raman data for the SHV-1 single crystal is consonant with the X-ray crystallographic results shown in Figure 4. The latter indicate that the C6 and C3 atoms in the acyl fragment are *trans* about the C5−N4 bond. The Raman data indicate that these are in fact a mixture of imine and *trans*-enamine present with the heavy atoms in the C6−C5−N4−C3 fragment in the

DOI: 10.1021/bi501197t
Biochemistry 2015, 54, 734−743

same position. The X-ray data at 1.37 Å resolution are unable to distinguish the tautomers.

DISCUSSION

Using Raman spectroscopy and X-ray crystallography, we are able to elucidate the inhibition mechanism of PSR-3-283A, a 6β-(hydroxymethyl)penicillanic acid sulfone, against SHV-1 class A β-lactamase. The slow tautomerization and deacylation observed are attributed to H-bonds from the additional 6-hydroxymethyl group.

Much work has been concentrated on the studies of 6-hydroxyalkylpenicillanate derivatives previously. They are found to display robust inhibitory activity against both class A and class C enzymes, such as TEM-1 and AmpC β-lactamases.[31,32] The Mobashery group proposes that 6-hydroxyalkypenicillanates inhibit class A and C β-lactamases depending on the approach direction of the deacylating water molecule.[33] 6α-Hydroxyalkylpenicillanates can effectively inhibit class A β-lactamases because the water molecule enters from the α direction, while 6β-hydroxyalkylpenicillanates can inhibit class C enzymes because the water molecule approaches from the β direction. Interestingly, PSR-3-283A, a 6β-(hydroxymethyl)-penicillanic acid sulfone, inhibits both class A and class C enzymes.[10] In particular, PSR-3-283A is able to improve the activity of piperacillin *in vitro* and *in vivo* against various β-lactamase producing microorganisms.[8] The 6α-(hydroxymethyl)penicillanic acid sulfone, on the other hand, did not show any inhibition against class A or C enzymes in the IC_{50} or MIC assays (unpublished screening work, Bethel and Bonomo). The X-ray structure of SHV-1 complexed with PSR-3-283A shows that the 6-hydroxymethyl group has two positions in the active site of SHV-1. It adopts two directions: one is H-bonded to the deacylation water molecule; the other points away from that water molecule. It is possible that these two directions mimic the positions of the water molecule in class A and C enzymes, respectively.

The presence of conformation 2 (Figure 4B) in the active site of SHV-1 may contribute to inhibition: the 6-CH_2OH in conformation 2 forms H-bonds with the −OH and C═O of S130. The S130 has been shown to participate in early events in β-lactamase catalysis by facilitating the protonation of the β-lactam nitrogen.[34] However, the species in conformation 2 may also undergo hydrolysis since the general base, E166, is free to utilize the catalytic water molecule to deacylate the enzyme, releasing the hydrolyzed product as *cis*-enamine. This outcome is supported by a population of *cis*-enamine detected by Raman spectroscopy in the solution reaction of SHV-1 with PSR-3-283A (Figure 3). The *cis*-enamine appears to be the favored outcome of both base and SHV-1 catalyzed hydrolysis.

Previously, Papp-Wallace et al.[10] detected not only imine and enamine species but also fragmentation and rearrangement in the reaction pathway of PSR-3-283A with TEM-1 and PDC-3, the AmpC of the pathogen *Pseudomonas aeruginosa*. Under our conditions of reacting SHV-1 with PSR-3-283A, at 23 ms, there appears to be approximately equal amounts of the enamine (species **5**/**6**, Scheme 2) and imine (species **3**, Scheme 2) intermediates (Figure 3). The accumulation of the imine indicates that the presence of the 6-hydroxymethyl group affects the tautomerization from imine to enamine. Kalp et al. showed that E166 in the active site of SHV-1 is involved in this tautomerization.[30] For imine to tautomerize to enamine, deprotonation at the C6 position is required. In wt SHV-1, deprotonation at C6 of the imine is mediated by E166 via an intervening water molecule. The importance of the C6 position is confirmed by the reaction between 6-D,D-sulbactam and SHV-1 (Figure S2, Supporting Information). Replacement of the hydrogen by deuterium at C6 leads to the accumulation of peak 1630 cm^{-1} (imine species), indicating that the imine−enamine tautomerization is slower due to the isotopic effect. The base hydrolysis of sulbactam also shows a slow transition from imine (1630 cm^{-1}, 3 min, Figure 2) to *cis*-enamine (1582 cm^{-1}, 60 min, Figure 2). However, in the presence of the SHV-1 enzyme, sulbactam can complete the imine−enamine transition within 23 ms using the E166 and the deacylation water molecule (Figure 3).

CONCLUSIONS

In summary, the 6β-hydroxymethyl penicillanic acid sulfone, PSR-3-283A, possesses key features such as enhanced affinity and a slow deacylation rate compared with the clinical inhibitor sulbactam. The addition of the 6β-hydroxymethyl group in sulbactam not only restores the inhibitory activity of the latter but also extends it to other class A and C β-lactamases. Raman studies in solution and the X-ray structure confirm the presence of a stable imine intermediate that forms H-bonds with a key residue, E166, and a deacylation water molecule. The latter interactions hinder water-mediated deacylation. The characteristic feature in PSR-3-283A is the quasi-stable imine; this is different from other effective class A and C β-lactamase inhibitors, such as tazobactam[4] and SA2-13,[7] which predominantly form stable *trans*-enamine species in the active site. The findings emphasize the roles of E166 and the deacylation water molecule. To impair the function of the glutamic acid (or analogous residues in other β-lactamases) or to displace or prevent the approach the deacylation water molecule is a critical challenge to the design of novel β-lactamase inhibitors.

ASSOCIATED CONTENT

Supporting Information

The ^1H NMR spectrum of sulbactam hydrolyzed by 1 M NaOH at different time points. This material is available free of charge via the Internet at http://pubs.acs.org.

Accession Codes

Coordinates and structure factors for the enzyme−inhibitor complexes have been deposited into the Protein Data Bank (PDB ID: 4R3B).

AUTHOR INFORMATION

Corresponding Author

*E-mail: prc5@case.edu.

Funding

This work was supported by NIH Grant GM54072 to P.R.C. Research reported in this publication was supported in part by funds from the National Institute of Allergy and Infectious Diseases of the National Institutes of Health under Award Numbers R01AI063517 and R01AI100560 to R.A.B. This study was also supported by funds or facilities provided by the Cleveland Department of Veterans Affairs, the Veterans Affairs Merit Review Program Award 1I01BX001974, and the Geriatric Research Education and Clinical Center VISN 10 to R.A.B. The content is solely the responsibility of the authors and does not represent the official views of the National Institutes of Health or the Department of Veterans Affairs.

Notes

The authors declare no competing financial interest.

DOI: 10.1021/bi501197t
Biochemistry 2015, 54, 734−743

■ ACKNOWLEDGMENTS

We thank Dr. Mary Barkley (Department of Chemistry, Case Western Reserve University) for the loan of the KinTek system. We also acknowledge the use of the High Performance Computing Cluster at Case Western Reserve University.

■ ABBREVIATIONS

MIC, minimum inhibitory concentration; ED_{50}, effective dose 50%; IC_{50}, inhibitory concentration 50%; EDTA, ethylenediaminetetraacetic acid; HEPES, (4-(2-hydroxyethyl)-1-piperazineethanesulfonic acid; NCF, nitrocefin

■ REFERENCES

(1) Abraham, E. P., and Chain, E. (1940) An enzyme from bacteria able to destory penicillin. *Nature 146*, 837.
(2) Ambler, R. P. (1980) The structure of beta-lactamases. *Philos. Trans. R. Soc. London, Ser. B 289*, 321−331.
(3) Drawz, S. M., and Bonomo, R. A. (2010) Three decades of beta-lactamase inhibitors. *Clin Microbiol Rev. 23*, 160−201.
(4) Kalp, M., Totir, M. A., Buynak, J. D., and Carey, P. R. (2009) Different intermediate populations formed by tazobactam, sulbactam, and clavulanate reacting with SHV-1 beta-lactamases: Raman crystallographic evidence. *J. Am. Chem. Soc. 131*, 2338−2347.
(5) Padayatti, P. S., Helfand, M. S., Totir, M. A., Carey, M. P., Carey, P. R., Bonomo, R. A., and van den Akker, F. (2005) High resolution crystal structures of the trans-enamine intermediates formed by sulbactam and clavulanic acid and E166A SHV-1 {beta}-lactamase. *J. Biol. Chem. 280*, 34900−34907.
(6) Padayatti, P. S., Helfand, M. S., Totir, M. A., Carey, M. P., Hujer, A. M., Carey, P. R., Bonomo, R. A., and van den Akker, F. (2004) Tazobactam forms a stoichiometric trans-enamine intermediate in the E166A variant of SHV-1 β-lactamase: 1.63 Å crystal structure. *Biochemistry 43*, 843−848.
(7) Padayatti, P. S., Sheri, A., Totir, M. A., Helfand, M. S., Carey, M. P., Anderson, V. E., Carey, P. R., Bethel, C. R., Bonomo, R. A., Buynak, J. D., and van den Akker, F. (2006) Rational design of a β-lactamase inhibitor achieved via stabilization of the trans-enamine intermediate: 1.28 Å crystal structure of wt SHV-1 complex with a penam sulfone. *J. Am. Chem. Soc. 128*, 13235−13242.
(8) Bitha, P., Li, Z., Francisco, G. D., Rasmussen, B. A., and Lin, Y. I. (1999) 6-(1-Hydroxyalkyl)penam sulfone derivatives as inhibitors of class A and class C beta-lactamases I. *Bioorg. Med. Chem. Lett. 9*, 991−996.
(9) Bitha, P., Li, Z., Francisco, G. D., Yang, Y., Petersen, P. J., Lenoy, E., and Lin, Y. I. (1999) 6-(1-Hydroxyalkyl))penam sulfone derivatives as inhibitors of class A and class C beta-lactamases II. *Bioorg. Med. Chem. Lett. 9*, 997−1002.
(10) Papp-Wallace, K. M., Bethel, C. R., Gootz, T. D., Shang, W., Stroh, J., Lau, W., McLeod, D., Price, L., Marfat, A., Distler, A., Drawz, S. M., Chen, H., Harry, E., Nottingham, M., Carey, P. R., Buynak, J. D., and Bonomo, R. A. (2012) Inactivation of a class A and a class C beta-lactamase by 6beta-(hydroxymethyl)penicillanic acid sulfone. *Biochem. Pharmacol. 83*, 462−471.
(11) Heidari Torkabadi, H., Che, T., Shou, J., Shanmugam, S., Crowder, M. W., Bonomo, R. A., Pusztai-Carey, M., and Carey, P. R. (2013) Raman Spectra of Interchanging β-Lactamase Inhibitor Intermediates on the Millisecond Time Scale. *J. Am. Chem. Soc. 135*, 2895−2898.
(12) Ke, W., Sampson, J. M., Ori, C., Prati, F., Drawz, S. M., Bethel, C. R., Bonomo, R. A., and van den Akker, F. (2011) Novel insights into the mode of inhibition of class A SHV-1 beta-lactamases revealed by boronic acid transition state inhibitors. *Antimicrob. Agents Chemother. 55*, 174−183.
(13) Rodkey, E. A., Drawz, S. M., Sampson, J. M., Bethel, C. R., Bonomo, R. A., and van den Akker, F. (2012) Crystal structure of a preacylation complex of the β-lactamase inhibitor sulbactam bound to a sulfenamide bond-containing thiol-β-lactamase. *J. Am. Chem. Soc. 134*, 16798−16804.
(14) Hujer, A. M., Hujer, K. M., and Bonomo, R. A. (2001) Mutagenesis of amino acid residues in the SHV-1 beta-lactamase: The premier role of Gly238Ser in penicillin and cephalosporin resistance. *Biochim. Biophys. Acta 1547*, 37−50.
(15) Che, T., Bethel, C. R., Pusztai-Carey, M., Bonomo, R. A., and Carey, P. R. (2014) The different inhibition mechanisms of OXA-1 and OXA-24 beta-lactamases are determined by the stability of active site carboxylated lysine. *J. Biol. Chem. 289*, 6152−6164.
(16) NCCLS. (2005) Performance standards for antimicrobial disk susceptibility testing, Fifteenth informational supplement. NCCLS document M100-S15. NCCLS, Wayne, PA.
(17) Carey, P. R. (2006) Raman crystallography and other biochemical applications of Raman microscopy. *Annu. Rev. Phys. Chem. 57*, 527−554.
(18) Otwinowski, Z., and Minor, W. (1997) Processing of X-ray diffraction data collected in oscillation mode. *Methods Enzymol. 276*, 307−326.
(19) Murshudov, G. N., Vagin, A. A., and Dodson, E. J. (1997) Refinement of macromolecular structures by the maximum-likelihood method. *Acta Crystallogr. D53*, 240−255.
(20) Emsley, P., and Cowtan, K. (2004) Coot: Model-building tools for molecular graphics. *Acta Crystallogr. D: Biol. Crystallogr. D60*, 2126−2132.
(21) Schuttelkopf, A. W., and van Aalten, D. M. (2004) PRODRG: A tool for high-throughput crystallography of protein-ligand complexes. *Acta Crystallogr. D: Biol. Crystallogr. D60*, 1355−1363.
(22) Kabsch, W. (1976) A solution for the best rotation to relate two sets of vectors. *Acta Crystallogr. A32*, 922−923.
(23) Broom, N. J. P., Farmer, T. H., Osborne, N. F., and Tyler, J. W. (1992) Studies on the Mechanism of Action of (5r)-(Z)-6-(1-Methyl-1,2,3-Triazol-4-ylmethylene)Penem-3-Carboxylic Acid (Brl-42715), a Potent Inhibitor of Bacterial Beta-Lactamase. *J. Chem. Soc., Chem. Commun.*, 1663−1664.
(24) Frisch, M. J., Trucks, G. W., Schlegel, H. B., Scuseria, G. E., Robb, M. A., Cheeseman, J. R., Montgomery, J. A., Jr., Vreven, T., Kudin, K. N., Burant, J. C., Millam, J. M., Iyengar, S. S., Tomasi, J., Barone, V., Mennucci, B., Cossi, M., Scalmani, G., Rega, N., Petersson, G. A., Nakatsuji, H., Hada, M., Ehara, M., Toyota, K., Fukuda, R., Hasegawa, J., Ishida, M., Nakajima, T., Honda, Y., Kitao, O., Nakai, H., Klene, M., Li, X., Knox, J. E., Hratchian, H. P., Cross, J. B., Bakken, V., Adamo, C., Jaramillo, J., Gomperts, R., Stratmann, R. E., Yazyev, O., Austin, A. J., Cammi, R., Pomelli, C., Ochterski, J. W., Ayala, P. Y., Morokuma, K., Voth, G. A., Salvador, P., Dannenberg, J. J., Zakrzewski, V. G., Dapprich, S., Daniels, A. D., Strain, M. C., Farkas, O., Malick, D. K., Rabuck, A. D., Raghavachari, K., Foresman, J. B., Ortiz, J. V., Cui, Q., Baboul, A. G., Clifford, S., Cioslowski, J., Stefanov, B. B., Liu, G., Liashenko, A., Piskorz, P., Komaromi, I., Martin, R. L., Fox, D. J., Keith, T., Al-Laham, M. A., Peng, C. Y., Nanayakkara, A., Challacombe, M., Gill, P. M. W., Johnson, B., Chen, W., Wong, M. W., Gonzalez, C., and Pople, J. A. (2003) *Gaussian 03*, revision C.02, Gaussian, Inc., Wallingford, CT.
(25) Anderson, A., and Savoie, R. (1965) Raman Spectrum of Crystalline and Liquid SO_2. *Can. J. Chem. 43*, 2271−2278.
(26) Song, Y., Liu, Z., Mao, H. K., Hemley, R. J., and Herschbach, D. R. (2005) High-pressure vibrational spectroscopy of sulfur dioxide. *J. Chem. Phys. 122*, No. 174511.
(27) Livermore, D. M., and Brown, D. F. (2001) Detection of beta-lactamase-mediated resistance. *J. Antimicrob. Chemother. 48* (Suppl 1), 59−64.
(28) Tonge, P. J., and Carey, P. R. (1989) Direct observation of the titration of substrate carbonyl groups in the active site of α-chymotrypsin by resonance Raman spectroscopy. *Biochemistry 28*, 6701−6709.
(29) Tonge, P. J., and Carey, P. R. (1990) Length of the acyl carbonyl bond in acyl-serine proteases correlates with reactivity. *Biochemistry 29*, 10723−10727.

DOI: 10.1021/bi501197t
Biochemistry 2015, 54, 734−743

(30) Kalp, M., Buynak, J. D., and Carey, P. R. (2009) Role of E166 in the imine to enamine tautomerization of the clinical β-lactamase inhibitor sulbactam. *Biochemistry 48*, 10196−10198.
(31) Maveyraud, L., Massova, I., Birck, C., Miyashita, K., Samama, J. P., and Mobashery, S. (1996) Crystal structure of 6α-(hydroxymethyl)penicillanate complexed to the TEM-1 β-lactamase from *Escherichia coli*: Evidence on the mechanism of action of a novel inhibitor designed by a computer-aided process. *J. Am. Chem. Soc. 118*, 7435−7440.
(32) Mourey, L., Miyashita, K., Swaren, P., Bulychev, A., Samama, J. P., and Mobashery, S. (1998) Inhibition of the NMC-A β-lactamase by a penicillanic acid derivative and the structural bases for the increase in substrate profile of this antibiotic resistance enzyme. *J. Am. Chem. Soc. 120*, 9382−9383.
(33) Golemi, D., Maveyraud, L., Ishiwata, A., Tranier, S., Miyashita, K., Nagase, T., Massova, I., Mourey, L., Samama, J. P., and Mobashery, S. (2000) 6-(hydroxyalkyl)penicillanates as probes for mechanisms of beta-lactamases. *J. Antibiot. (Tokyo) 53*, 1022−1027.
(34) Atanasov, B. P., Mustafi, D., and Makinen, M. W. (2000) Protonation of the beta-lactam nitrogen is the trigger event in the catalytic action of class A beta-lactamases. *Proc. Natl. Acad. Sci. U. S. A. 97*, 3160−3165.

DOI: 10.1021/bi501197t
Biochemistry 2015, 54, 734−743